A Novel Method Based on Monte Carlo for Simulation of Variable Resolution X-ray CT Scanner: Measurement of System Presampling MTF

H. Arabi, A.R. Kamali Asl

Abstract—The purpose of this work is measurement of the system presampling MTF of a variable resolution x-ray (VRX) CT scanner. In this paper, we used the parameters of an actual VRX CT scanner for simulation and study of effect of different focal spot sizes on system presampling MTF by Monte Carlo method (GATE simulation software). Focal spot size of 0.6 mm limited the spatial resolution of the system to 5.5 cy/mm at incident angles of below 17º for cell#1. By focal spot size of 0.3 mm the spatial resolution increased up to 11 cy/mm and the limiting effect of focal spot size appeared at incident angles of below 9º. The focal spot size of 0.3 mm could improve the spatial resolution to some extent but because of magnification non-uniformity, there is a 10 cy/mm difference between spatial resolution of cell#1 and cell#256. The focal spot size of 0.1 mm acted as an ideal point source for this system. The spatial resolution increased to more than 35 cy/mm and at all incident angles the spatial resolution was a function of incident angle. By the way focal spot size of 0.1 mm minimized the effect of magnification non-uniformity.

Keywords—Focal spot, Spatial resolution, Monte Carlo simulation, Variable resolution x-ray (VRX) CT.

I. Introduction

THE capability of computed tomography (CT) to provide three-dimensional and high contrast images, has made it a powerful method of diagnostic imaging. The field of view (FOV) and spatial resolution are two main factors of CT scanners. Clinical CT scanners have relatively large FOV of 50 cm for imaging of whole body and spatial resolution of 2-3 cy/mm [1], [2] . Decrease in object size has no effect on spatial resolution of the clinical CT scanners. On the other hand, micro-CT scanners are appropriate for imaging of small objects. Such scanners have spatial resolution of up to 100 cy/mm however, the FOV of them is only a few centimeters [2], [3].

A CT scanner that can provide the advantages of both clinical and micro-CT scanner is highly demanded. In variable resolution x-ray (VRX) CT scanner, the spatial resolution can be changed according to the object size [4], [5]. The main innovation in such scanner is that by angulation of the detector

H. Arabi is with Radiation Dept. of Shahid Beheshti University, Tehran, Iran (corresponding author to provide phone: +98 21 29903187; fax: +98 21 22431780; e-mail: H.A.Hosein.Arabi@gmail.com).

A. R. Kamali Asl (PhD) was with Radiation Dept. of Shahid Beheshti University, Tehran, Iran (e-mail: A_R_Kamali@yahoo.com).

with respect to the incident x-ray beam, the apparent cells width in object plane will decrease and the detector resolution will rise consequently. This technique provides great increase in the detector resolution and by changing the detector angle with respect to the x-ray beam, variable resolution will be achieved. By VRX CT scanner, objects are imaged at highest possible spatial resolution according to their sizes or FOV. Small objects are imaged at high spatial resolution and small FOV; on the contrary large objects are image at relatively low spatial resolution and large FOV.

In VRX CT systems the main factor that limits the spatial resolution is the influence of the focal spot. By angulation of the detector, the spatial resolution improvement is due to increase in detector resolution but the influence of geometrical unsharpness due to the focal spot remains constant. To reach acceptable spatial resolution in VRX CT systems, the limiting effect of focal spot on spatial resolution should be precisely studied. To fulfill this aim, we used the numerical values of parameters of an actual VRX CT scanner for simulation and calculation of line spread function (LSF). The effect of different focal spot sizes of 0.6 mm, 0.3 mm, and 0.1 mm on the spatial resolution of the system was studied. By focal spot size of 0.6 mm, the spatial resolution could not rise more than 5.5 cy/mm and by 0.3 mm, spatial resolution stopped at 11 cy/mm. The focal spot size of 0.1 mm was ideally small for this system and totally eliminated the influence of geometrical unsharpness due to the focal spot effect on the spatial resolution of the system.

II. Materials and methods

A. VRX CT scanner

Fig. 1 shows a typical VRX CT scanner that includes a dual-arm VRX detector. The two detector's arms can rotate around a common pivotal point (vertex). The dual-arm VRX detector is preferable for its left-right symmetry, lower magnification variations, and higher uniformity of detector performance from one end of detector to the other [6]. On the diagram, the scanner's FOV is represented by the circle and the object plane is at the center of the FOV circle.

The x-ray source is placed at a distance SV (source-vertex) from the vertex and SO is distance of x-ray source from the center of object plane. α and θ are respectively opening half angle and incident angle.

World Academy of Science, Engineering and Technology
International Journal of Biomedical and Biological Engineering
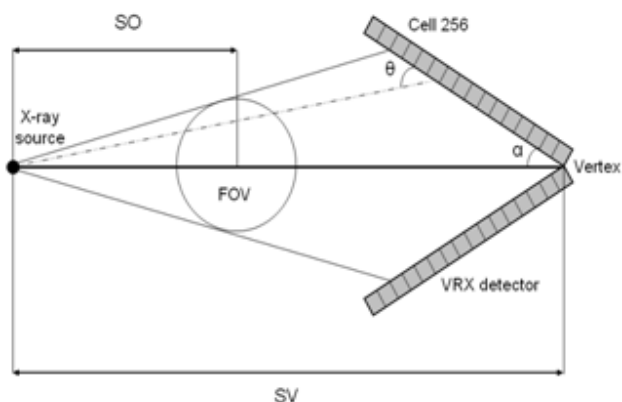Vol:4, No:8, 2010

Fig. 1 Schematic diagram of a variable resolution x-ray (VRX) CT scanner.

B. System presampling MTF

The MTF is a standard measure of spatial resolution for the imaging systems. The response of the system to the sinusoidal inputs in frequency domain is called MTF [7]. The System presampling MTF is a valuable measure of spatial resolution for the digital imaging systems [8]-[10]. The system presampling MTF consists of two main parts: detector presampling MTF and geometric unsharpness MTF.

$$\text{MTF}_{\text{system presampling}} = \text{MTF}_{\text{detector presampling}} \times \text{MTF}_{\text{geometric unsharpness}} \quad (1)$$

The detector presampling MTF is the inherent resolution of one cell in the detector and includes only detector aperture, x-ray scattering, and light diffusion in detection medium. Therefore, the detector presampling MTF describes the resolution of discrete detector without influence of geometric unsharpness, sampling, and image reconstruction [11]. Measuring the line spread function (LSF) is experimentally usual for evaluation of the detector presampling MTF. The LSF is defined as a pixel intensity distribution in the image of a line object of unit intensity [7]. The detector presampling LSF is measured by moving wire or slit method for 1 dimensional discrete detectors [12]-[14]. After measurement of LSF, the corresponding MTF can be computed as

$$\text{MTF}(f) = k|F\{\text{LSF}(x)\}| \quad (2)$$

Where $F\{\}$ is the Fourier transform function, x and f represent the spatial and frequency coordinates, and k is a normalization constant.

Once the detector presampling LSF is modeled, the detector presampling MTF is then computed.

The geometric unsharpness MTF refers to loss in image details due to effects of finite size of x-ray tube focal spot and system magnification [8]. The width of the focal spot when projected onto the object plane determines the geometric unsharpness due to influence of focal spot [8]. This width at the object plane is equals

$$S(x) = \frac{A(x) \times (M-1)}{M} \quad (3)$$

where A is the focal spot size and M is the system magnification. The geometric unsharpness MTF due to influence of focal spot is obtain by

$$\text{MTF}_{\text{geometric unsharpness}}(f) = k|F\{S(x)\}| \quad (4)$$

The system magnification also determines the projected detector presampling LSF on the object plane (LSF(Mx)). Hence, the system presampling MTF that is the total influence of detector resolution and focal spot size at the object plane is obtained by

$$\text{MTF}_{\text{system presampling}} = \text{MTF}_{\text{geometrical unsharpness}}(f) \times \text{MTF}_{\text{detector presampling}}(f/M)$$

C. VRX CT scanner parameters

To evaluate the system presampling in a VRX CT scanner , we used a geometrical model of VRX CT scanner based on an actual system designed and built by R. Melnyk et al [15]. The VRX CT scanner consists of dual-arm VRX detector (like Fig. 1). Each arm includes 12 modules of 24 cells. Two outer lead separators are placed at the module's ends and cells in every module are separated by inner lead separators. Cells are composed of Cadmium tungstate (CdWO$_4$) that reflective paint (Al$_2$O$_3$) coats between scintillator crystals (cells) and the separators in a module. Table 1 gives the main parameters of the VRX detector.

In the actual VRX CT scanner 256 out of 288 cells are assumed to image an object that are the active cells. Based on Schematic diagram (Fig. 1) and geometrical parameters of the actual VRX CT scanner that are given in Table 1, the relevant geometrical parameters of the system (FOV, opening half angle, incident angle, and system magnification) were computed.

TABLE I
Parameters of VRX detector and VRX CT scanner [15]

Number of cells	576
Cell material	CdWO$_4$
Separator material	Pb
Reflective paint material	Al$_2$O$_3$
Cell width	0.79 mm
Inner separator width	0.10 mm
Outer separator width	0.18 mm
Reflective paint width	0.05 mm
Cell height	20.14 mm
Cell thickness	3.00 mm
Source-vertex distance	150 cm
Source-vertex distance	106 cm
Number of active cells per arm	256
Number of reference cells per arm	32
Active arm length	25.617 cm

D. Monte Carlo simulation

GATE 4.0 software was used for the simulation. This software is a dedicated Monte Carlo code for simulation of the PET and SPECT [16]. But GATE 4.0 provides proper tools for simulation of CT scanners. GATE 4.0 has predefined functions and geometries that they facilitate the procedure of the simulation.

To simulate the detector presampling MTF, we used the actual VRX detector parameters in Table 1 and the features of Melnyk's model [15]. Only one arm of the VRX detector was considered because there is left-right symmetry. In the model,

World Academy of Science, Engineering and Technology
International Journal of Biomedical and Biological Engineering
Vol:4, No:8, 2010

288 cadmium tungstate (CdWO$_4$) cells and inner cells separators of lead composed one detector module. There were gaps between the inner separators and the cells corresponding to a reflective paint in the actual VRX detector. There was an aluminum oxide (Al$_2$O$_3$) base behind the cells.

A polychromatic beam x-ray source was used to instead of slit or wire for simulation of LSF. The spektr toolbox was used to generate the source spectra [17]. For the source spectrum generation, we used aluminum (Al) filtration of 3 mm and the optimum x-ray tube voltage for tissue phantom according to Melnyk experimental measurement [15]. The voltage of the x-ray tube changed nonlinearly from 40 kVp to 125 kVp as the FOV increased from 1 cm to 40 cm. The beam thickness was equal to 10 cm at all opening half angles.

For modeling and measuring the system presampling MTF, 15 different opening half angles were chosen for assessment of the total trend of system presampling MTF. At each of these opening half angles, first, the detector presampling LSF was measured three times for cell#1 , cell#128 (middle active cell), and cell#256 (last active cell). The number of samples for simulation of each LSF was 512. We used the Move command in GATE code for 512 samples of LSF in each run. Each movement was equal to 1/20 of the projected cell width. The number of photons for simulation of each sample was 30,000 to ensure the statistical error of less than 0.3%.

After obtaining the detector presampling MTF, the system magnification and geometrical unsharpness due to effect of the focal spot size were computed for measuring the system presampling MTF. To investiGATE the effect of focal spot size at system presampling MTF, in each opening half angle different focal spot sizes were computed and compared.

III. RESULTS

Table 2 represents the detector presampling MTF of the VRX detector at some incident angles. This is provided to validate the result of model in GATE software with the earlier published practical measurement and simulation [15].

The system presampling MTF of four different focal spot sizes at opening half angle of 25º for cell#128 (middle active cell) is shown in Fig. 2. Since in the actual VRX CT scanner the focal spot size is 0.6 mm, in the following figures the corresponding curves are of the special interest. At the opening half angle of 25°, the focal spot size has almost no effect on the spatial resolution of the system.

Even focal spot size of 0.8 has no significant effect on the spatial resolution of the system but the focal spot sizes of above 1 mm can deteriorate the spatial resolution at this opening half angle. By reducing the opening half angle, the spatial resolution of the system becomes more limited by the influence of the focal spot size.

TABLE II
RESULTS OF OUR MODEL BY GATE SIMULATION SOFTWARE WITH PRACTICAL AND SIMULATION RESULTS OF THE REFERENCE [15]

Opening half angle (deg)	Incident angle (deg)		Spatial resolution (cycle/mm)	
	Reference	Modeled	Reference	Modeled
53.43 (cell#128)	57.55	57.50	1.45	1.44
21.9 (cell#1)	21.91	21.91	3.3	3.3
10.6 (cell#256)	12.76	12.73	5.5	5.4
5.26 (cell#256)	6.34	6.33	11	10.8
2.63 (cell#283)	3.24	3.23	22	21.8
1.31 (cell#283)	1.62	1.61	42	41.7

At the opening half angle of 10°, the spatial resolution of the system is limited by the influence of focal spot (Fig. 3). Decreasing the focal spot size from 0.6 mm to 0.3 mm can increase the spatial resolution more than 1 cy/mm. As the opening half angle decreases, consequently the spatial
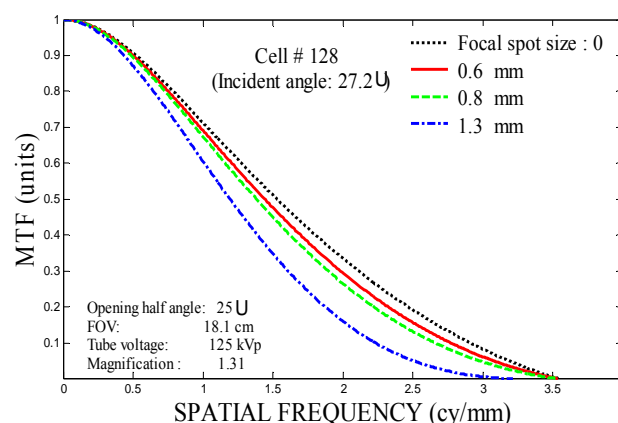

Fig. 2 Spatial resolution of the system at opening half angle of 25° with different focal spot sizes for middle active cell (cell#128).

resolution of the system is expected to increase, but the influence of focal spot (0.6 mm) limits the spatial resolution of the system to constant value (Fig. 4). Even with focal spot size
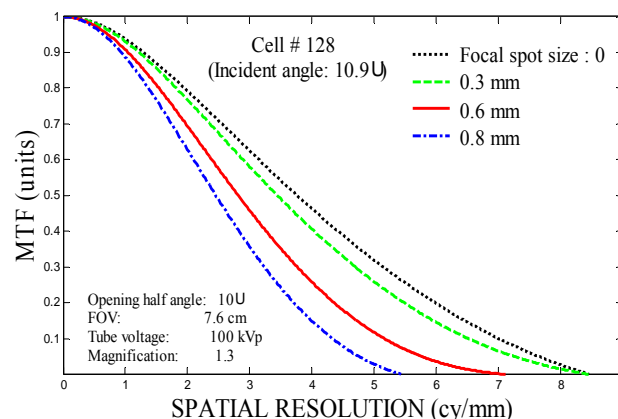

Fig 3. Spatial resolution at opening half angle of 10°. Focal spot size of 0.3 mm is ideal at this angle for middle active cell (cell#128).

World Academy of Science, Engineering and Technology
International Journal of Biomedical and Biological Engineering
Vol:4, No:8, 2010

of 0.3 mm, the spatial resolution of the system at opening half angle of 4º cannot reach 14 cy/mm. An ideally small focal spot size is needed to obtain high spatial resolution at small opening half angles. The influence of focal spot on the spatial resolution of the system is not similar for all the detector cells at each opening half angle. Since there is magnification non-uniformity from one end of the detector arm to the other, the effect of focal spot is different for each cell. Because of angulation of the detector arms in VRX CT scanner, the cell#1 has largest system magnification and last active cell (cell#256) has the lowest magnification.

This magnification non-uniformity depends on the length of the detector and opening half angle. The study of Fig. 5 and Fig. 6 shows how different system magnification for cell#1 and cell#256 causes huge difference in system presampling MTF at small incident angles.

Focal spot size of 0.1 mm is sufficiently small for this system that has no effect on the spatial resolution of the system. Since focal spot size of 0.1 mm acts as an ideal focal spot, it minimizes the influence of geometrical unsharpness on spatial resolution of the system (Fig. 7). Therefore, the spatial resolution of the system is totally determined by detector resolution. The difference in presampling system MTF for cell#1 and cell#256 stems from effect of magnification non-uniformity on detector resolution. The effect of magnification non-uniformity is less effective on detector resolution than geometrical unsharpness. Hence the resolution difference between the cell#1 and cell#256 greatly decreased by focal spot size of 0.1 mm [18].

IV. DISCUSSION

In a VRX CT scanner by angulation of the detector and consequently decreasing the apparent cell size in object plane, the spatial resolution of the system will increase. This resolution improvement is due to increase in detector resolution and the influence of the geometrical unsharpness remains constant for all opening half angles . At large opening half angles, where the detector resolution is lower than geometrical unsharpness, changing the focal spot size has no significant influence on the spatial resolution of the system. Because the main parameter that determines the spatial resolution of the system is detector resolution, by decreasing the opening half angle the spatial resolution of the system will increase as a function of the incident angle. But at small opening half angles (below 17º for cell#1) by focal spot size of 0.6 mm, the geometrical unsharpness is the main factor that determines the spatial resolution of the system, so it limits the spatial resolution to the constant value and resolution will not increase as a function of the incident angle.

When the detector resolution is lower than geometrical unsharpness, cell#1 has the highest resolution because it has maximum system magnification and cell#256 has lowest resolution. On the contrary, when the geometrical unsharpness is the dominant factor that determines the spatial resolution of the system, cell#1 has lowest resolution and cell #256 has highest resolution. So study of cell#1 is a good benchmark for investigation of focal spot effect.

Reducing the focal spot size from 0.6 mm to 0.3 mm has no signification effect on the spatial resolution of the system at
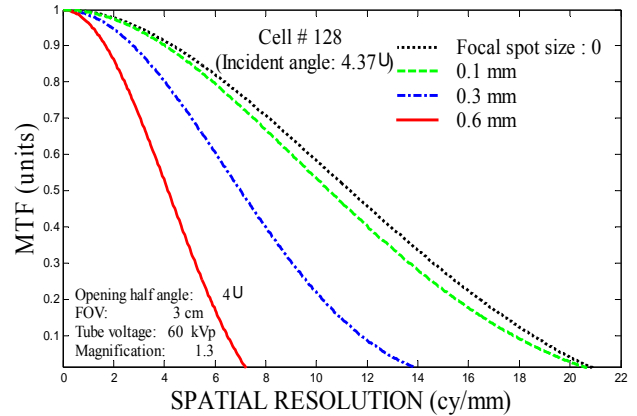

Fig. 4 At opening half angle of 4°, the focal spot sizes of 0.6 mm and 0.3 mm greatly limit the spatial resolution of the system.

incident angles of larger than 17º for cell#1. But for incident angles of below this value, focal spot size of 0.3 has two advantages. First, the spatial resolution increased twice as high as with focal spot size of 0.6 mm. Second, the limiting effect of focal spot appeared at lower incident angles (under 9°). It means that the spatial resolution of the system changes in larger range as a function of incident angle. Even by focal spot size of 0.3 mm, the resolution of the system at small incident angles is dominantly under influence of the geometrical unsharpness. So the magnification non-uniformity causes great difference between cell#1 and cell#256 (up to10 cy/mm). Focal spot size of 0.1 mm eliminates the effect of geometrical unsharpness due to the effect of focal spot on the spatial resolution of the system. So at all incident angles, the spatial resolution is determined by detector resolution and changes as a function of incident angle.
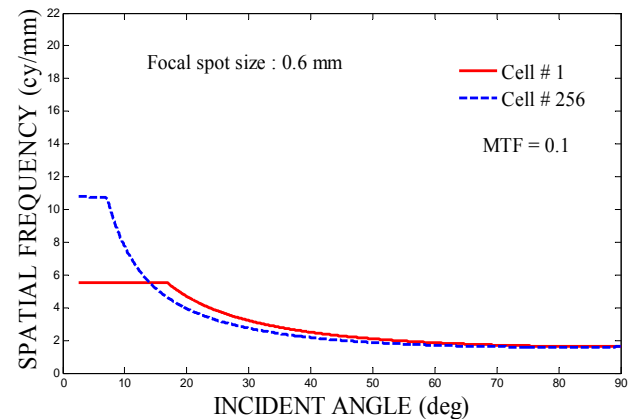

Fig. 5 The effect of focal spot size of 0.6mm on the spatial resolution of the cell#1 and cell#256.

V. CONCLUSION

In a VRX CT scanner, by decreasing the opening half angle, the detector resolution will increase as a function of the incident angle. But the spatial resolution of the system stops at constant value due to focal spot limitation. The focal spot size of 0.6 mm limits the spatial resolution at the value of 5.5 cy/mm in incident angle of 17º for cell#1.Reducing the focal

World Academy of Science, Engineering and Technology
International Journal of Biomedical and Biological Engineering
Vol:4, No:8, 2010

spot size under 0.6 mm has no considerable effect on the spatial resolution of the system for incident angles of larger than 17º, but at small incident angles, by focal spot size of 0.3 mm, the spatial resolution rises up to 11 cy/mm. Since there is magnification non-uniformity along the VRX detector, the difference between the spatial resolution of cell#1 and cell#256 (last active cell) is more than 6 cy/mm for focal spot size of 0.6 mm and 10 cy/mm for focal spot size of 0.3mm. Focal spot size of 0.1 mm acts as an ideal point source for this system and has three advantages. First, the spatial resolution increases to more than 35 cy/mm. Second, the spatial resolution of the system at all incident angles is the function of incident angle and third, it minimizes the difference between resolution of cell#1 and cell#256.
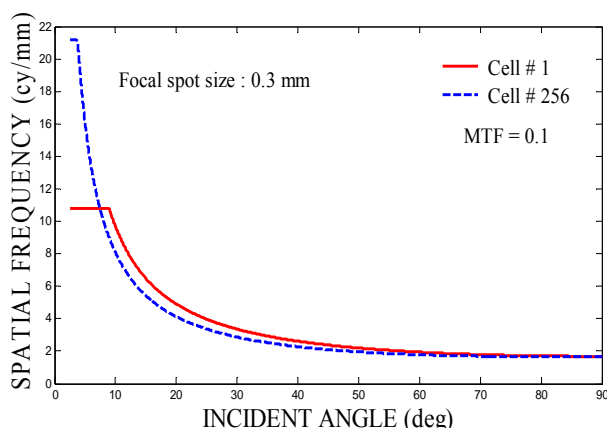
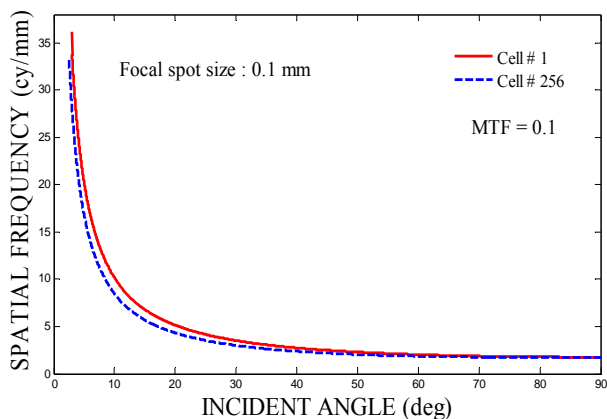Fig. 6 The effect of focal spot size of 0.3 mm on the spatial resolution of the cell#1 and cell#256.

Fig. 7 Focal spot size of 0.1 mm is ideally small for the VRX CT scanner. It totally eliminates the influence of focal spot.

ACKNOWLEDGMENT

REFERENCES

[1] J. Beutel, H. L. Kundel, and R. L. van Metter, *Handbook of Medical Imaging*. Physics and Psychophysics 1. SPIE Press Bellingham, 2000.

[2] G. Wang, S. Zhao, H. Yu, C. Miller, P. Abbas, B. Gantz, S. Lee, and J. Rubinstein, "Design, analysis and simulation for development of the first clinical micro-CT scanner," *Acad. Radiol.*, vol. 12, pp. 511–525, 2005.

[3] A. Sasov and D. van Dyck, "Desktop x-ray microscopy and microtomography," *J Microsc*, vol. 191, pp. 151–158, 1998.

[4] F. A. DiBianca, V. Gupta, and H. D. Zeman, "A variable resolution x-ray detector for computed tomography: I. Theoretical basis and experimental verification," *Med Phys*, vol. 27:8, pp. 1865-1874, 2000.

[5] F. A. DiBianca, P. Zou, L. M. Jordan, J. S. Laughter, H. D. Zeman, and J. Sebes, "A variable resolution x-ray detector for computed tomography: II. Imaging theory and performance," *Med Phys*, vol. 27:8, pp. 1875-1880, 2000.

[6] F. A. DiBianca, R. Melnyk, C. N. Duckworth, S. Russ, L. M. Jordan, and J. S. Laughter, "Comparison of VRX CT scanners geometries," *Proc. SPIE,* vol. 4320, pp. 627-635, 2001.

[7] K. Rossmann, "Point spread-function, line spread-function, and modulation transfer function. Tools for the study of imaging systems," *Radiology*, vol. 93, pp. 257–272, 1969.

[8] J. L. Lancaster, "Physics of Medical X-Ray Imaging." http://ric.uthscsa.edu/personalpages/lancaste/DI II.html. Accessed 20 jan 2008.

[9] M. L. Giger and K. Doi, "Investigation of basic imaging properties in digital radiography. I. Modulation transfer function," *Med. Phys*, vol. 11, pp. 287-295 1984.

[10] H. Fujita, K. Doi, and M. L. Giger, "Investigation of basic imaging properties in digital radiography. 6. MTFs of II-TV digital imaging systems," *Med Phys*, vol. 12, (), pp. 713- 720 1985.

[11] J. T. Dobbins, "Effects of undersampling on the proper interpretation of modulation transfer function, noise power spectra, and noise equivalent quanta of digital imaging systems," *Med Phys*, vol. 22, pp. 171–181, 1995.

[12] H. Fujita, D. Y. Tsai, T. Itoh, K. Doi, J. Morishita, K. Ueda, and A. Ohtsuka, "A simple method for determining the modulation transfer function in digital radiography," *IEEE Trans Med Imaging*, vol. 11, pp. 34–39 1992.

[13] J. T. Dobbins, D. L. Ergun, L. Rutz, D. A. Hinshaw, H. Blume, and D. C. Clark, "DQE(f) of four generations of computed radiography acquisition devices," *Med Phys*, vol. 22, pp. 1581–1593, 1995.

[14] E. Samei, N. T. Ranger, J. T. I. Dobbins, and Y. Chen, "Intercomparison of methods for image quality characterization. I. Modulation transfer function," *Med Phys,* vol. 33, pp. 1454–1465, 2006.

[15] R. Melnyk and F. A. DiBianca, "Modeling and measurement of the detector presampling MTF of a variable resolution x-ray CT scanner," *Med Phys*, vol. 34:3, pp. 1062-1075, 2007.

[16] S. Jan, G. Santin, D. Strul, S. Staelens, K. Assie, D. Autret et al "GATE: a simulation toolkit for PET and SPECT," *Physics in medicine and biology*, vol. 49:19, pp. 4543-4561, 2004.

[17] J. H. Siewerdsen, A. M. Waese, D. J. Moseley, S. Richard, and D. A. Jaffray, "Spektr: a computational tool for x-ray spectral analysis and imaging system optimization," *Med Phys*, vol. 31:11, pp. 3057-3067, 2004.

[18] H. Arabi, A. R. Kamali Asl, S. M. R. Aghamiri "The Effect of focal spot size on the spatial resolution of variable resolution x-ray CT scanner," *Iranian Journal of Radiation Research,* To be published.